Impact of Noise on Electrocardiographic Imaging Resolution with Zero Order Tikhonov Regularization and L-Curve Optimization

Rubén Molero[1], Jana Reventós-Presmanes[1,2], Ivo Roca[2], Lluís Mont[2], Andreu M. Climent[1], María S. Guillem[1]

[1]ITACA Institute, Universitat Politècnica de València, València, Spain
[2]Department of Arrhythmias, Hospital Clínic de Barcelona, Barcelona, Spain

Abstract

Electrocardiographic Imaging (ECGI) allows computing the electrical activity in the epicardium by inverting the electrical propagation matrix, which can be solved by regularizing this ill-posed problem. The objective of this study is to evaluate the effects of noise on the signals in the selection of the regularization parameter (λ) by zero-order Tikhonov and L-curve optimization.

Fourteen atrial fibrillation (AF) simulations were used for computing the ECGI with different noise levels (3, 10, 20, 30, and 40dB). Signals of real cardiac rhythms were also used to compute the ECGI (3 AF, 2 atrial flutters, 3 atrial pacing, 3 atrial sinus rhythm and 3 ventricular tachycardia). For simulations and patients, maximum L-curve curvature and λ were obtained and compared.

The maximum curvature of the L-curve, noise level and optimal λ correlated for AF simulations. Higher levels of noise resulted in smaller curvatures of the L-curve and the selection of higher values of λ, reducing the amplification of noise when computing ECGI. Real cardiac signals of AF presented similar results in curvature and λ as the higher values of noise explored in simulations (3dB, $\lambda > 10^{-6}$, curvature < 1). The noise of the signal proportionally affects to the reconstruction of ECGI. The given results show a methodology to obtain trustable ECGI maps based on the shape of the L-curve optimization.

1. Introduction

Electrocardiographic Imaging (ECGI) allows estimating the epicardial activity by using the information of Body Surface Potential Mapping (BSPM) recordings and information relative to the geometry of the torso and the heart. In previous studies, ECGI has shown to estimate reliable epicardial potentials when compared with intracardiac mapping data [1]. Nevertheless, epicardial potential estimation based on BSPM data remains an ill-posed problem that strongly depends on different sources of noise (i.e., signals artifacts, geometry, regularization methodology). During the last decades, multiple approaches have been used for obtaining the optimal ECGI reconstruction, with zero-order Tikhonov and L-curve optimization one of the most used approaches by the ECGI community [2]. This method works especially well for noisy signals such as atrial fibrillation (AF), because it allows minimizing the effects of the noise by providing an smooth solution when regularization parameters (λ) are explored in the adequate range [3]. However, this method presents some limitations under noise conditions that do influence the selection of the optimal solution [4], since the shape of the L-curve is affected. The objective of this study is to evaluate the impact of different levels of noise on the L-Curve shape and regularization parameter selection by using simulated electrograms and real ECGI signals for different cardiac rhythms.

2. Material and Methods

2.1. Simulations

Fourteen atrial fibrillation simulations of 10 seconds of duration were created using the same cardiac geometry and different AF episodes. A realistic 3D model of the atrial anatomy composed by 284.578 nodes and 1.353.783 tetrahedrons was used for creating the simulations [5]. Variation of currents were introduced in $I_{k,ACH}$, I_{K1}, I_{Na} and ICaL to simulate electrical remodeling and allow the maintenance of fibrillation. Fibrotic tissue was modeled by disconnecting a percentage of nodes between 20% and 60% and scar tissue by disconnecting 100% of nodes in the scar region. The system of differential equations was solved by using Runge–Kutta integration based on a graphic processors unit (NVIDIA Tesla C2075 6G), [5]. AF was induced by implementing an S1 S2 protocol, with the S2 stimulus applied at different locations in the atria, thus producing different AF patterns.

A torso mesh geometry of 771 nodes was used for all simulations. The forward problem was then computed to

obtain the body surface potentials by multiplying the transfer matrix and the computed electrograms. Noise was then added at 5 different levels (3, 10, 20, 30, and 40 dB signal-to-noise ratios). Baseline was then subtracted by a 1 Hz high-pass filter followed by a low pass filter of 40 Hz.

2.2. Patient Data

Signals from 14 patients with different cardiac rhythms (3 AF, 2 atrial flutters (AFl), 3 atrial pacing (AP), 3 atrial sinus rhythm (SR) and 3 ventricular tachycardia (VT) were registered using Body Surface Potential Mapping with 64 electrodes. Torso geometries and lead positioning of each patient were reconstructed by photogrammetry and cardiac geometry was reconstructed using MRI/CT scans. BSPM signals were band-pass filtered between 1 and 40 Hz to improve the signal-to-noise ratio. AF signals of 1 minute length were selected and QRS was cancelled using a PCA approach [6]. For non-fibrillating rhythms a single beat was manually selected for the ECGI calculation. For illustrating the inverse reconstruction, local activation times of an example of SR and VT were computed. Furthermore, phase singularities of an example of AF were computed as described in [7].

2.3. Inverse Problem Computation

For the inverse problem calculation of simulations and real data, zero-order Tikhonov regularization was used together with the L-curve optimization for selecting the regularization parameter. This regularization allows estimating the epicardial potentials by minimizing equation 1:

$$\left||Ax-b|\right|_2^2+\lambda\left||Lx|\right|_2^2 \quad (1)$$

where the first term corresponds to the norm of the solution, x are the epicardial potentials, b the surface potentials and A the transfer matrix, which was computed by using the Boundary Element Method. The second term of the equation is the residual norm of the solution multiplied by the identity matrix L. This second term is multiplied by the regularization parameter λ that is chosen to minimize the equation by finding the maximum curvature of the two terms of equation 1 [4].

Values of λ and maximum curvatures of the simulations were extracted and adjusted to a polynomial to relate the selection of λ based on the curvature of the L-curve. Furthermore, confidence intervals of the adjusted equation based on the possible values of curvature were established with a confidence level of 0.05.

3. Results

3.1. ECGI regularization in AF simulations

In Fig. 1, results of the regularization parameters and maximum curvatures of L-curve for AF simulations are presented for the different added noise levels. As it can be observed, there is an inverse relationship between noise level and optimal regularization parameter ($\lambda = 10^{-10}$ for 40 dB SNR vs. $\lambda = 10^{-5}$ for 3dB SNR). The noise level is also inversely related with the maximum curvature at the corner of the L curve. The observed relationship allows defining an expected regularization parameter, described in equation 2.

$$\lambda = 10^{-1.83*max.\ curvature-4.01} \quad (2)$$

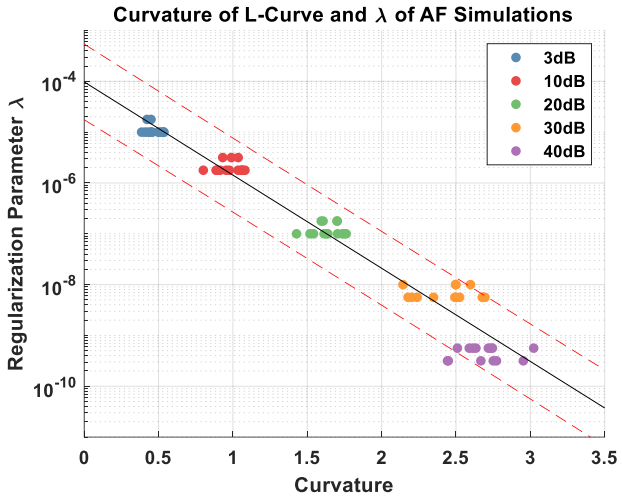

Figure 1. Curvature and regularization parameter λ resultant from the inverse problem calculation of atrial fibrillation simulations with different levels of noise added. Adjusted equation 2 is represented (black line) with confidence intervals (α = 0.05, red dashed line).

In Fig. 2, an example of the L-curves and their curvature for each of the explored λ values is presented. Scenarios with high noise levels are bounded to higher residual errors, which results in a more vertical-shape L-curve and low curvatures at the corner (Fig. 2B), whereas scenarios with low SNR reach smaller residual errors and steeper corners of the L-curve.

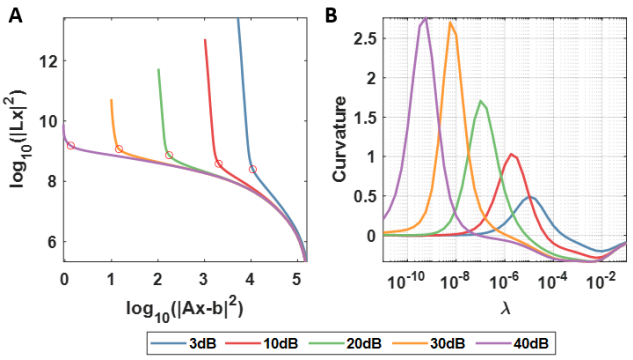

Figure 2. Examples of L-curves (A) and their curvature (B) of an atrial fibrillation simulation for different noise levels.

3.2. ECGI regularization in patient data

Regularization parameters and curvatures of signals from patients were extracted and compared with the simulation values shown in Fig. 3. Results showed that for real signals, maximum curvature and λ have similar relationship as observed in simulations, with higher values of curvature related to smaller values of λ. Furthermore, signals expected to be nosier as AF signals (blue crosses in Fig. 3) presented lower values of curvature and higher values of λ, ($\lambda > 10^{-6}$), with the subsequent smoother solutions that will attenuate the noise present in the data. Signals of other rhythms expected to present higher signal-to-noise ratios (i.e., SR or VT) do reach larger curvatures and lower λ values. Besides, most of the observed λ and curvatures, fit in the estimated intervals of confidence, validating the relationship also in real patients.

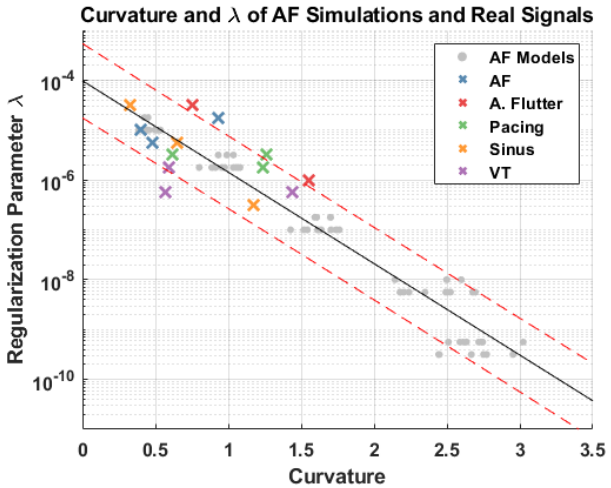

Figure 3. Curvature and regularization parameter from the inverse problem calculation of atrial fibrillation simulations and real signals of atrial fibrillation, atrial flutter, atrial pacing, sinus rhythm and ventricular tachycardia.

In Fig 4. three sample cases are depicted. During sinus rhythm and VT activation is quite homogeneous. In sinus rhythm (Fig. 4.A) the activation starts from the sinoatrial node, whereas activation times in VT showed a reentrant activation in the right ventricle (purple region of Fig, 4B). During AF, multiple reentrant sites are observed, as illustrated in the rotor histogram in Fig. 4C. In addition, an example of L-curves and curvatures of real ECGI signals is presented in Figure 4. BSPM signals were normalized in order to compare the shapes and curvatures for the different cardiac rhythms. As it can be observed in Fig 4D, AF signals presented larger residual errors, more vertical L-curves and smaller curvatures at the corner of the L-curve (Fig. 4E) than SR, and VT signals.

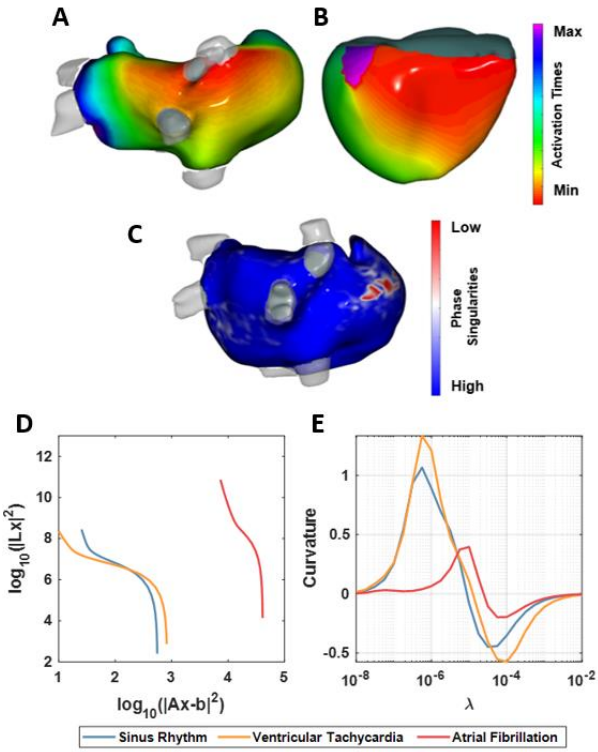

Figure 4. Representation of the epicardial maps activation times of the examples of sinus rhythm (A) and ventricular tachycardia (B) and rotor histogram of an atrial fibrillation signal (C). L-curves (D) and their curvature (E) of the represented signals from patients of SR, VT, and AF.

4. Discussion

In the present study, a relationship between the noise level present in BSPM signals and both the curvature at the corner of the L-curve and the optimal λ selection has been evaluated. We have shown that the noise level is inversely related with the curvature at the corner of the L-curve. From our results we can define the range of λ values that should be acceptable based on the curvature at the corner

of L-curve: λ values below our defined ranges should be avoided because they will result in solutions without sufficient noise attenuation [3][8].

Curvature and λ values of simulations and real cardiac signals overlapped with the observed values on simulations. L-curves obtained from real patient BSPM signals presented curvatures within noise levels from 3 to 20 dB, which is consistent with noise levels in real recorded signals. In fact our results suggest that our signals may present noise levels above 30 dB in all cases and, therefore, λ values under 10^{-7} should not be considered in the parameter space search, which, in turn, is consistent with our prior observations on AF signals [3]. On the other hand, we were expecting to find a clear separation between AF and the other rhythms, with a clear separation between AF signals -assumed to be similar to high noise level scenarios- and non-AF signals -assumed to be similar to lower noise levels- but we didn't observe separated clusters. AF signals, however, were found to present consistently lower curvatures at the corner of the L-curve and larger λ values were selected. This observation could be explained by the presence of other sources of noise, such as geometrical errors, that may have a large impact on ECGI reconstruction on top of the electrical noise of the recorded signals.

5. Conclusion

The noise level present on BSPM signals do have an impact on the reconstruction of ECGI signals when applying Tikhonov regularization and L-Curve optimization methods. The noise level is directly related with the curvature at the corner of the L-curve and the selected regularization parameter. Results show that the noise of the signal can be estimated based on the Inverse Problem resolution. Finally, our results allow us to propose a confidence range for the regularization parameter search based on the level of curvature observed in the L-curve and therefore obtain trustable solutions of ECGI maps for non-invasive physiological interpretation of epicardial activity.

Acknowledgements

This work was supported by: Instituto de Salud Carlos III and Ministerio de Ciencia, Innovación y Universidades (supported by FEDER Fondo Europeo de Desarrollo Regional PI17/01106, PID2020-119364RB-100), Agencia Estatal de Investigación (RYC2018-024346B-750), and Generalitat Valenciana (ACIF/2020/265).

Conflicts of Interest

MS. Guillem and AM. Climent are co-founders and stakeholders of Corify Care S.L. I. Roca is Lecturer Honoraria per Abbott and Biosense.

References

[1] M. Rodrigo et al., "Non-Invasive Assessment of Complexity of Atrial Fibrillation: Correlation with Contact Mapping and Impact of Ablation," *Circ. Arrhythmia Electrophysiol.*, vol. 13, no. 3, e007700, Feb. 2020.

[2] J. Salinet et al., "Electrocardiographic Imaging for Atrial Fibrillation: a Perspective from Computer Models and Animal Experiments to Clinical Value," *Front. Physiol.*, vol. 12, pp. 1–23, Apr. 2021.

[3] R. Molero, et al., "Electrocardiographic Imaging in Atrial Fibrillation: Selection of the Optimal Tikhonov-Regularization Parameter," *Comput. Cardiol*., vol. 48, pp. 1-4, Sept. 2021.

[4] P. C. Hansen and D. P. O'Leary, "The Use of the L-Curve in the Regularization of Discrete Ill-Posed Problems," *SIAM J. Sci. Comput.*, vol. 14, no. 6, pp. 1487–1503, Nov.1993.

[5] M. Rodrigo et al., "Technical considerations on phase mapping for identification of atrial reentrant activity in direct- And inverse-computed electrograms," *Circ. Arrhythmia Electrophysiol.*, vol. 10, no. 9, p. e005008, 2017.

[6] F. Castells, et al., "Estimation of atrial fibrillatory wave from single-lead atrial fibrillation electrocardiograms using principal component analysis concepts," *Med. Biol. Eng. Comput*., vol. 43, no. 5, pp. 557–560, Oct. 2005.

[7] C. Fambuena-Santos, et al., "An Evaluation on the Potential Clinical Outcome Prediction of Rotor Detection in Non-Invasive Phase Maps," *Comput. Cardiol.*, vol. 48, pp. 1–4, Sept. 2021.

[8] C. Hansen, "Analysis of discrete ill-posed problems," *Soc. Ind. Appl. Math*, vol. 34, no. 4, pp. 561–580, Dec. 1992.

Address for correspondence:

Rubén Molero Alabau
ITACA. Edificio 8G acceso B. Universitat Politècnica de València. Camino de Vera s/n. 46022 Valencia, Spain.
rumoal1@itaca.upv.es